Physica A 392 (2013) 6389–6399

Contents lists available at ScienceDirect

Physica A

journal homepage: www.elsevier.com/locate/physa

Study of capillary network directionality and irrigation of hypoxic tissue in an angiogenesis lattice model

Belén Moglia [a,b], Nara Guisoni [a,*], Ezequiel V. Albano [a,b]

[a] Instituto de Física de Líquidos y Sistemas Biológicos (CONICET, UNLP), 59 Nro 789, 1900 La Plata, Argentina

[b] Departamento de Física, Facultad de Ciencias Exactas, Universidad Nacional de La Plata, La Plata, Argentina

HIGHLIGHTS

- We propose a simplified lattice model for capillary network formation.
- Hypoxic tissue and a growing capillary network can produce growth factors.
- We consider an inhibition mechanism due to irrigation of hypoxic tissue.
- Directionality of the network is more evident when local growth factors are absent.
- A better irrigation is achieved when the inhibition mechanism is considered.

ARTICLE INFO

Article history:
Received 30 January 2013
Received in revised form 7 August 2013
Available online 20 August 2013

Keywords:
Angiogenesis
Lattice model
Stochastic model
Monte Carlo simulation
Hypoxic tissue
Capillary network

ABSTRACT

To shed light on the understanding of the angiogenesis process, we study a simplified lattice model for the capillary network formation between an existing blood vessel and an initially hypoxic tissue. We consider that the cells of the tissue surface can release growth factors that will diffuse, leading to the formation of new capillaries that ultimately arrive at the tissue. Additionally, we consider the local production of growth factors by the growing capillary network. We also propose the existence of an inhibition mechanism at the hypoxic surface, i.e., a fixed number of neighboring sites of an already irrigated site of the hypoxic tissue stop releasing growth factors due to the arrival of nutrients. Particularly, the goal of this work is to study the effect of the release of local growth factors and the inhibition mechanism on properties such as the directionality of the growing network and the irrigation of the hypoxic tissue. Therefore we propose the quantification of these two relevant features for angiogenesis modeling. We establish a relationship between the model behavior without the release of local growth factors in the presence of the inhibition mechanism and a normal angiogenesis process. In this situation, the model gives a directional capillary network and a good irrigation of the hypoxic tissue. On the other hand, for a large number of released local growth factors in the absence of the inhibition mechanism, the model could be appropriate for the description of tumor angiogenesis. In this case, the model provides a rather small directionality for the growing structure, with a worse degree of irrigation of the hypoxic tissue, as well as a more tortuous capillary network with many closed branches and loops.

1. Introduction

Angiogenesis is the complex physiological process that results in the growth of new blood vessels from preexisting ones. It involves the growth, the branching, and the extension of these blood vessels (capillaries) until the hypoxic tissue. Under

* Corresponding author. Tel.: +54 2214233283; fax: +54 2214257317.
E-mail addresses: naraguisoni@gmail.com, naraguisoni@conicet.gov.ar (N. Guisoni).

0378-4371/$ – see front matter © 2013 Elsevier B.V. All rights reserved.
http://dx.doi.org/10.1016/j.physa.2013.08.016

normal circumstances, angiogenesis not only supports the growth and development of tissues, but also helps repair and heal injured ones. This is a complex process governed by a balance of several pro-angiogenic and anti-angiogenic factors. Among the identified substances that promote angiogenesis, the so-called vascular endothelial growth factor (VEGF) and the basic fibroblast growth factor (bFCF) seem to be the most prevalent [1–3]. On the other hand, substances such as thrombospodin, angiostatin, endostatin, etc., are the best known inhibitors of the angiogenesis process [4].

Nearly 40 years ago, cancer researchers started to focus their attention on angiogenic factors when it was established that dormant tumors might release this kind of substance in order to foster their own growth. In fact, in his pioneer work, J. Folkman [5] argues that some tumors, unable to grow beyond 2–3 mm^3 in size due to the lack of enough nutrients, can produce and release angiogenic growth factors that, after diffusion toward vascular endothelial cells, may induce the formation of new vessels and the subsequent vascularization of the tumor [6]. Nowadays it is well known that the disruption of the delicate balance between pro- and anti-angiogenic factors is related to a large number of diseases. In fact, many human diseases are driven by persistently up-regulated angiogenesis, which generates an over-irrigation [7]. In some nonmalignant processes, such as keloid formation, angiogenesis is prolonged but still self-limited [8], whereas in tumor angiogenesis this process continues indefinitely without control [9]. Therefore, the control of the angiogenic switch has an enormous potential for the generation of new therapies [9–13].

Under these circumstances, the study and understanding of angiogenesis have become the focus of growing activity. Apart from well-established experimental methods, more recently the mathematical modeling and simulation of angiogenesis have received increasing attention [14]. In fact, by using this alternative approach one can gain an insight into the underlying mechanisms involved in these complex biological processes and contribute to a more comprehensive description. An overview of recent work on the mathematical modeling of angiogenesis reveals that several strategies have already been used. The continuous approach assumes that the relevant ingredients of the process, such as the density of new capillaries, the concentration of angiogenic factors, etc., can be described by means of a set of coupled partial differential equations [15–17]. In this case, one deals with continuous quantities treated in a mean-field fashion. On the other hand, discrete models at the mesoscopic scale have also been proposed. Usually, these models are based on a set of simple rules inspired by biological mechanisms and often containing stochastic ingredients at the level of individual cells and molecules [17–19]. Besides, hybrid models, which include the discrete approach at the cellular level and continuous equations for the diffusion at the extracellular level, have been reported to describe angiogenesis [20–29].

Within this broad context, the aim of this paper is to study the capillary network obtained from a simplified lattice model by means of Monte Carlo computer simulations. Our model is based on an early work by Gazit et al. [18] who proposed to study the scale-invariant behavior of normal and tumor capillary network formation through simplified models. They consider that growth begins at a single central seed and that growth factors diffuse from points at a certain distance from the structure, in a circular geometry in $d = 2$ dimensions [18]. In order to obtain a compact structure, observed experimentally in a normal subcutaneous capillary network [30], Gazit et al. compare two hypotheses for network formation. As one possibility, they consider that the main source of growth factors is the growing structure itself, that is, besides the release of growth factors from points distant from the structure, there is a release of local growth factors. As an alternative scenario, they also consider a low interaction probability between growth factors and the growing structure. The authors show that both mechanisms can lead to the formation of the compact capillary network observed experimentally [18]. It is worth noting that the model proposed by Gazit et al. derives from the classic diffusion limited aggregation model (DLA) [31].

In this paper we study a model for the formation of new capillaries between an hypoxic tissue and a neighboring blood vessel [18]. The growing of the capillary network is induced by growth factors released by the hypoxic tissue, as well as, by a local amplification of this signal. We made an extension of the model proposed by Gazit et al. [18]. In this way, we include an inhibition mechanism, i.e., a fixed number of neighboring sites of an already irrigated site of the hypoxic tissue stop releasing growth factors due to the arrival of nutrients. Besides, we propose a geometry that allows the study of the directionality of the growing network. Particularly, our task in this paper is to study the effect of the release of local growth factors and the inhibition mechanism on properties such as the directionality of the growing network and the degree of irrigation of the hypoxic tissue, in order to obtain a better description and understanding of the angiogenesis process.

The manuscript consists of the description of the model and the simulation method (Section 2), the presentation and discussion of the results (Section 3), and the statement of the conclusions (Section 4).

2. Description of the model and the simulation method

Simulations are performed in a two-dimensional square lattice by considering samples of width L (horizontal axis) and length M (vertical axis). The first column on the leftmost-hand side of the sample is assumed to be taken by an existing blood vessel (see Fig. 2), composed of endothelial cells. Also, a fraction of the last column at the rightmost-hand side of the sample, having a length m, is assumed to be taken by the part of the tissue that is initially hypoxic (see Fig. 2). Hereafter, we use $m \sim M/3$ because in this work we are interested in studying how the capillary network grows toward a hypoxic tissue of length smaller than that of the vessel. The sites between the blood vessel and the tissue surface are considered as extracellular matrix.

The closest distance between the hypoxic tissue and the vessel is the sample width L, while the structure of the bulk of tissue, which is irrelevant for the purpose of the present work, is no longer considered. Despite the great complexity of angiogenesis, we consider that the cells of the hypoxic tissue can release only the vascular endothelial growth factor

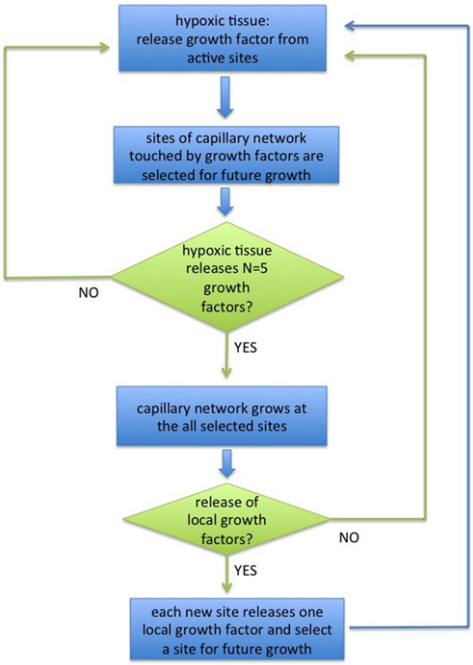

Fig. 1. (Colors on line.) Flowchart of the model for the release of growth factors and growing of the capillary network (the inhibition mechanism is not represented). The hypoxic tissue releases growth factors that can touch the capillary network for future growth. Just after the release of $N = 5$ growth factors the marked sites are incorporated to the capillary network (delay mechanism). When the local amplification is present each new site of the growing network releases one LGF. More details in the text.

(VEGF), which is considered one of the most important substances that promotes angiogenesis [18]. We also consider that the cells of the tissue surface can be in two possible states: active, when they can release growth factors (GF's) that will promote angiogenesis, and inhibited for the release of growth factors. Therefore, GF's are released from randomly selected active sites of the hypoxic tissue, generating a diffusion field that presents higher concentration near the tissue surface. The diffusion of the GF's through the extracellular matrix toward an existing vessel is modeled by considering the GF's as random walkers [32], as made before for other biological phenomena such as bacterial growth in a diffusion field generated by the nutrient concentration [33].

At the beginning, when a GF released by an active site of the hypoxic tissue touches the existing vessel, the site of contact is selected for further growth. Just after the release of a fixed number N of GF's from the hypoxic tissue, all the selected sites in contact with the growing network actually become part of it. This delay mechanism intends to represent, in a simplified way, the fact that the cell expends some time between the arrival of a GF, which will initiate several processes in the cell related to the degradation of the extracellular matrix, proliferation and diffusion of endothelial cells, etc., and that the cell effectively contributes to the growth of the vascular network, represented in this model by a new site in the growing network. We also consider that each new site that becomes part of the growing network can release one local growth factor (LGF), which causes the additional signaling of one of its neighboring sites for further growth, generating a local amplification of the signal generated by the GF's released by the hypoxic tissue [18]. In this way, the capillary network grows due to both the GF's released from the hypoxic tissue and the local amplification of the LGF's (see the flowchart in Fig. 1).

Due to the growth process, which proceeds from the release of GF's by the hypoxic surface of the tissue, the capillary network ultimately gets in contact with sites of the tissue surface (see Fig. 2). The sites of the tissue already irrigated by blood coming from the new capillary network are considered inhibited for further release of GF's, since these sites do not represent a hypoxic tissue anymore. Additionally, we considered a local inhibition mechanism, i.e., a number of neighboring sites on both sides of the already irrigated site of the hypoxic tissue also become inhibited and stop releasing GF's. In the model, this type of neighboring inhibition mechanism represents the regulation of the hypoxic tissue toward the release of GF's due to the arrival of nutrients.

Hereafter, when the local amplification is present we assume that each site of the growing network touched by a growth factor released by the hypoxic tissue is able to release one LGF. The absence of LGF's in our model means that LGF's are not released. Also, in order to account for the effect of the neighboring inhibition mechanism, hereafter we assume that when one capillary touches the hypoxic tissue, 5 of their sites become inhibited for the release of GF's, i.e. the touched site and the two neighboring sites located at each side of the touched one. Hereafter, we also consider that the hypoxic tissue releases $N = 5$ GF's during a single growing event of the network. Fig. 1 shows the flowchart of a single time step of the simulation, which includes the release of $N = 5$ GF's from the hypoxic tissue, the incorporation of the selected sites to the growing

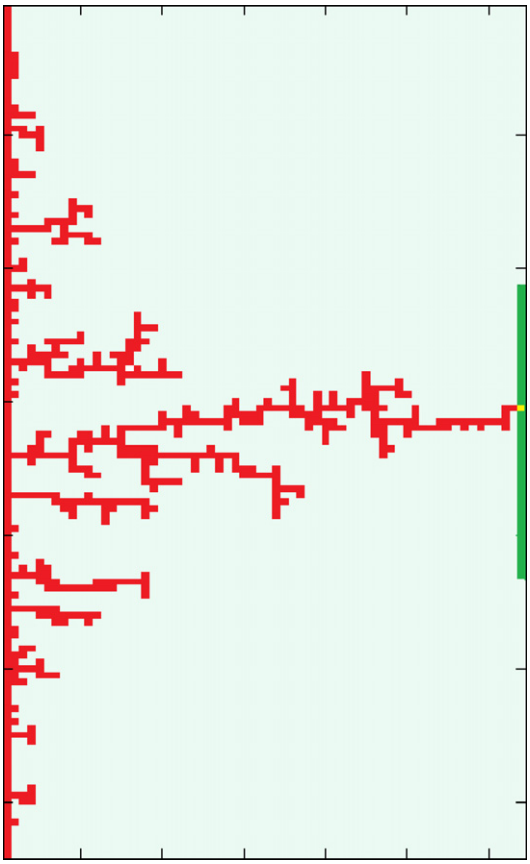

Fig. 2. (Colors on line.) *Sketch of the simulation geometry*. On the leftmost side one has an existing blood vessel (solid red line), while on the rightmost side the solid green line represents the surface of the hypoxic tissue. Growth factors are released from the hypoxic tissue and induce the growth of the capillary networks (shown in red). The sketch corresponds to an actual simulation stopped when the first capillary gets in contact with the hypoxic tissue. The site touched by the capillary (yellow) becomes inhibited for the release of GF's. Sample of width $L = 64$, length $M = 128$ and length of the hypoxic tissue $m = 44$. More details in the text.

capillary network (both from GF's of this time step and LGF's of the previous time step) and the release of the corresponding LGF's. Each simulation run stops after a fixed number N_f of capillaries have arrived at the tissue surface. Results discussed in the next section are averaged over a number n_S of different individual runs. It is worth mentioning that we adopt free boundary conditions since the GF's that move away from the vessel do not contribute to the growing structure, and therefore they are irrelevant for the purpose of the work. Also, as it follows from the definition of the model, one has that GF's never diffuse over the capillary network, but only through the extracellular matrix.

Several important aspects of the angiogenesis process, such as tissue growth, cellular death, nutrient distribution and consumption by the cells, vessel remodeling, etc., are disregarded in our simplified model. It should also be mentioned that the simulation of the angiogenesis process in two dimensions has the advantage that both the modeling and the analysis are simpler, as can be seen from the number of theoretical works performed in $d = 2$ dimensions [15,16,18,20,21,25,26,28,29]. Furthermore, experiments can be performed in two dimensions in order to be directly compared with theoretical predictions. In fact, Gazit et al. [18] compare simulation results with images of capillary networks obtained from the inoculation of tumor cell suspensions in the striated muscle of a mouse's back after the implantation of a special transparent quasi-two-dimensional device [30].

3. Results

In order to gain insight into the structure of the patterns formed upon angiogenesis, in Fig. 3 we show typical snapshot configurations obtained in the presence or absence of both the release of local growth factors and the inhibition mechanism. Fig. 3(A) and (B) (upper panels) correspond to simulations performed when the release of local growth factors is not considered, whereas Fig. 3(C) and (D) (lower panels) show the influence caused by the release of local growth factors. Fig. 3(A) and (C) (left panels) were obtained in the absence of a neighboring inhibition effect, i.e., only the sites of the tissue in contact with the capillary network are inhibited for further release of GF's, while in Fig. 3(B) and (D) (right panels) the neighboring inhibition effect is present. For all cases we stop the simulation when $N_f = 23$ capillaries touch the hypoxic tissue.

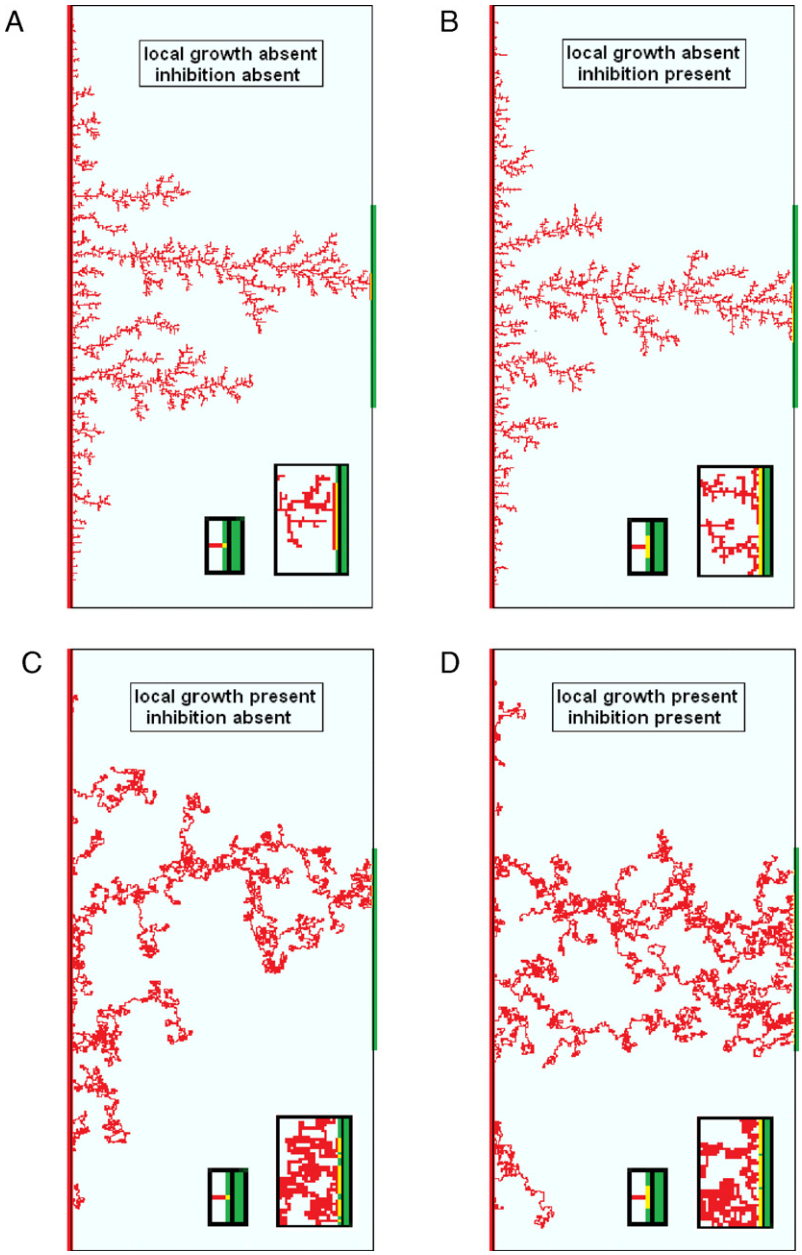

Fig. 3. (Colors on line.) *Typical snapshot configurations for comparing the effect of the release of LGF's and the inhibition mechanism*. The upper figures (A and B) correspond to snapshot configurations without the release of LGF's, whereas the lower snapshot configurations (C and D) correspond to configurations where LGF's are released. In the left panels (A and C) the inhibition mechanism is absent, while in the right panels (B and D) it is present. Insets show an enlargement of the region where the capillary network touches the tissue. Small insets show the inhibition mechanism: sites inhibited for the release of GF's are represented in yellow. For all figures we stop the simulation when $N_f = 23$ capillaries touch the hypoxic tissue. Simulation conditions: $L = 256$, $M = 512$, and $m = 172$. More details in the text.

When the growth factors are released only by the hypoxic tissue (upper panels), the capillary network appears to preferentially touch the sites of the center of the hypoxic tissue, both in the absence or presence of the inhibition mechanism (Fig. 3(A) and (B), respectively). However, the presence of LGF's (lower panels, Fig. 3(C) and (D)) seems to blur the directionality of the growing capillary network, since the release of growth factors from the growing capillary network distorts the gradient generated by the tissue. Besides, when local growth factors are present (lower panels), the growing network seems to be more dense and tortuous as compared with the situation where they are absent (upper panels). Also, from Fig. 3, one can see that the extension of the hypoxic tissue touched by the capillaries seems to be bigger for the case with the inhibition effect (right panels, Fig. 3(B) and (D)), particularly when LGF's are released (Fig. 3(D)).

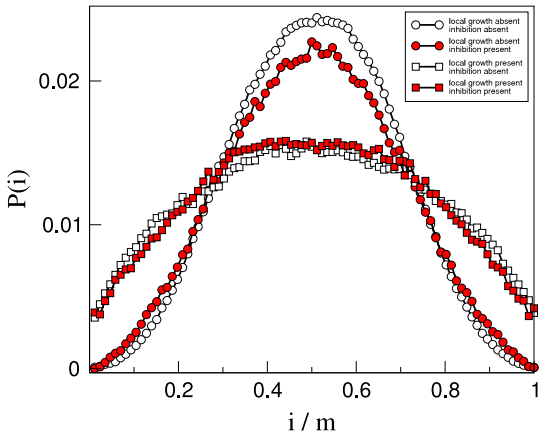

Fig. 4. (Colors on line.) *Directionality of the growing capillary network*. Probability $P(i)$ that a site i of the hypoxic tissue becomes touched by a capillary. Comparing four situations: with and without LGF's (squares and circles, respectively) and in the presence and in the absence of a neighboring inhibition mechanism (filled red symbols and empty symbols, respectively), for the same simulation conditions ($L = 128$, $M = 256$, $m = 86$, $N_f = 12$ and $n_S = 10{,}000$).

A more quantitative analysis about the influence of both the LGF's and the neighboring inhibition mechanism on the directionality of the growing capillary network can be obtained from the measurement of the probability $P(i)$ that a site i of the tissue surface ($i \leq m$) becomes touched by a capillary, for a fixed number N_f of capillaries that arrive at the tissue, as shown in Fig. 4.

From Fig. 4 one observes preferential irrigation around the center of the hypoxic tissue (that is, around the site $i = m/2$) in the absence of LGF's, while a more spread irrigation is achieved when LGF's are considered. The neighboring inhibition mechanism seemingly does not play an important role in the directionality of the capillary network, although for the case when LGF's are not considered, the growing network appears to be a little more directional in the absence of the neighboring inhibition mechanism (curve with empty circles in Fig. 4).

Additional insight into the dynamic growth of the capillary network can be gained by computing the vertical density of capillary sites ($\rho(y)$) during the growth process. Considering a site (x, y) of the lattice (x being the horizontal direction, with $1 \leq x \leq L$, and y the vertical direction, with $1 \leq y \leq M$) let us define a variable occupation $\eta(x, y)$, with $\eta(x, y) = 0$ if the site is composed of extracellular matrix, and $\eta(x, y) = 1$ if it is occupied by a capillary site. Therefore we have

$$\rho(y) = \frac{1}{L} \sum_{x=1}^{L} \eta(x, y). \tag{1}$$

In Fig. 5 one can see $\rho(y)$ in the absence of LGF's, which corresponds to case A of Fig. 3. The simulation times t used in Fig. 5 are before the arrival of the capillary network at the hypoxic tissue, therefore the inhibition mechanism is not relevant (case B of Fig. 3). Fig. 5(A) shows that essentially one has a Gaussian distribution of capillary sites around the symmetry axis of the sample (that is, the horizontal axis placed at $y = M/2$) for all times. In order to obtain reasonable statistics, averages are taken over $n_S = 100,000$ different runs, always for the same simulation conditions.

The width of the distribution is larger at early times, indicating that at the beginning of the angiogenic process the GF's arrive almost homogeneously at the already existing blood vessel. However, when the number of released GF's increases, the width of the Gaussian decreases indicating preferential growth of capillaries around the symmetry axis (Fig. 5(A)). The dependence of both the width (W) and the height (H) of the Gaussians can be fitted and plotted against time (inset of Fig. 5(B)). The observed curves can be well fitted by simple polynomials, namely,

$$W = A_1 t^{\beta} + A_2, \tag{2}$$

and

$$H = B_1 t^{\alpha} + B_2, \tag{3}$$

where t is the simulation time, β and α are exponents associated with the width and the height of the Gaussians, respectively, and the remaining symbols are constants. The best fits of the data yield $A_1 = -1.7 \times 10^{-6}$, $A_2 = 0.57$, $\beta = 1.18$, $B_1 = 5.3 \times 10^{-8}$, $B_2 = 0.0095$, and $\alpha = 1.38$. By normalizing the Gaussian with the aid of Eqs. (2) and (3), one can obtain a collapsed plot of the data from Fig. 5(A), as shown in the main panel of Fig. 5(B).

Fig. 6 shows the behavior of $\rho(y)$ in two situations: with and without the release of LGF's (cases C and A of Fig. 3, respectively). We recall that the presence or absence of the inhibition mechanism (cases D and B of Fig. 3) cannot be considered, because we are analyzing the growth of the network before the arrival of the capillary network at the hypoxic tissue. Here, one observes a difference in the time behavior of the distributions: the highest and narrowest distribution

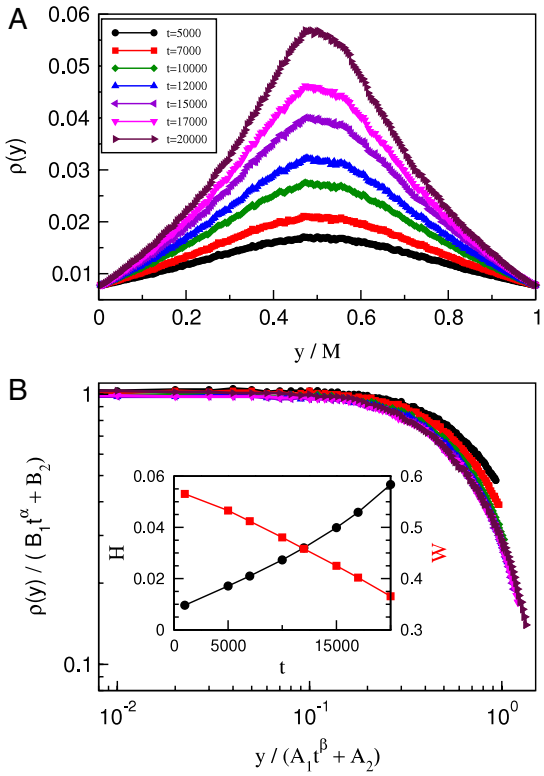

Fig. 5. (Colors on line.) *Vertical density of capillary sites.* (A) Vertical density of capillary sites ($\rho(y)$) in the absence of LGF's, as a function of y/M, during the growth process for different simulation times t (values indicated in the figure). Figure (B) shows scaled plots of the data presented in (A). More details in the text. The inset of (B) shows the dependence of both the width (W) and the height (H) of the Gaussians presented in (A) versus the simulation time t. For all figures we have $L = 128$, $M = 256$ and $n_S = 100{,}000$. The length of the hypoxic tissue (m) and N_f are not relevant since the data presented here are related to simulation times before to the arrival of the capillary network at the hypoxic tissue.

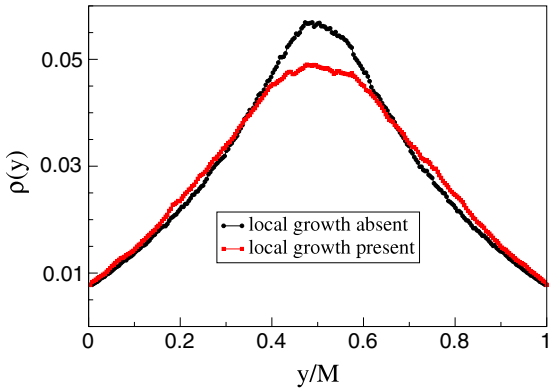

Fig. 6. (Colors on line.) Directionality of the growing capillary network before the arrival at the hypoxic tissue. Vertical density of capillary sites ($\rho(y)$) obtained for the cases with and without the release of LGF's (squares and circles, respectively). Both results are obtained for the same simulation conditions ($L = 128$, $M = 256$, and $n_S = 100{,}000$).

corresponds to the case where LGF's are not released. This scenery is confirmed by the fitting of the Gaussians for different simulation times (not shown here for the sake of space) with the aid of Eqs. (2) and (3), where the best fits of the data when the LGF's are present, yield $A_1 = -0.018$, $A_2 = 0.46$, $\beta = 0.42$, $B_1 = 2.0 \times 10^{-5}$, $B_2 = 0.0067$, and $\alpha = 1.25$. The values obtained when the LGF's are absent were presented in the previous paragraph (Fig. 5(A)). Since the constant A_1 is negative, the bigger value of the exponent β obtained for the case without the release of LGF's, implies that the width of the Gaussians becomes narrow more quickly, and therefore in this case one has a more directional growing network. Therefore, the directionality of the growing network observed when the capillaries touch the hypoxic tissue (Fig. 4) can also be seen before to the arrival of the vessel at the hypoxic tissue (Fig. 6).

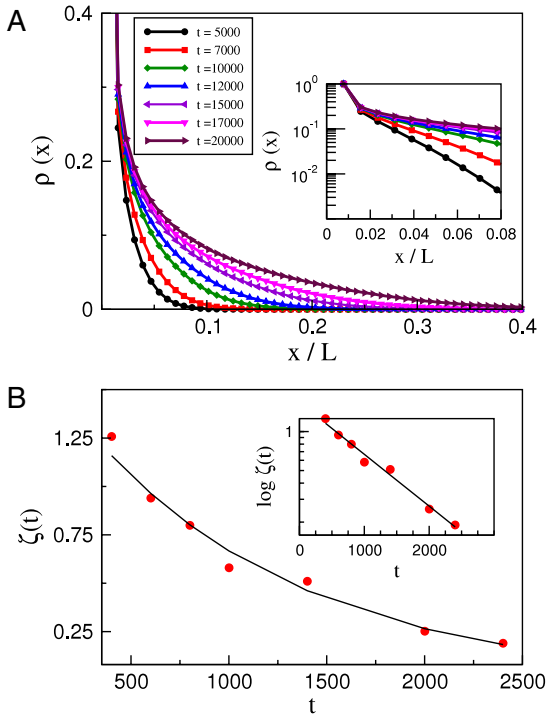

Fig. 7. (Colors on line.) *Horizontal density of capillary sites.* (A) Horizontal density of capillary sites ($\rho(x)$) in the absence of LGF's, as a function of x/L, during the growth process for different simulation times t (values indicated in the figure). The inset shows the log–linear plots of the data shown in (A) for small distances of the initial blood vessel ($x/L \leq 0.08$). (B) Characteristic distance of $\rho(x)$ ($\zeta(t)$) as a function of the time simulation. The inset shows the log–linear plot of data presented in (B). For all figures we have $L = 128$, $M = 256$ and $n_S = 100{,}000$. The length of the hypoxic tissue (m) and N_f are not relevant since the data presented here are related to simulation times before to the arrival of the capillary network at the hypoxic tissue.

Additionally, one can compute the horizontal density of capillary sites ($\rho(x)$) during the growth process, i.e., the fraction of sites occupied by the capillaries as a function of the distance between the initial blood vessel and the surface of the tissue,

$$\rho(x) = \frac{1}{M}\sum_{y=1}^{M}\eta(x, y). \tag{4}$$

Fig. 7(A) shows the behavior of $\rho(x)$ in the absence of LGF's. A figure obtained in the presence of LGF's is quite similar, so that it is not shown here for the sake of space. One observes a remarkable decrease of the horizontal density with the distance to the blood vessel, as indicated by the straight lines, obtained for small distances ($x/L \leq 0.08$), in the log–linear plots shown in the inset of Fig. 7(A).

One can also calculate the characteristic distance of the horizontal density of capillary sites, ζ, obtained from the fitting of $\rho(x)$,

$$\rho(x) = A e^{-\frac{x}{\zeta}}, \tag{5}$$

where A is a constant. In Fig. 7(B) we show that ζ as a function of time exhibits an exponential decrease, as can be seen in the inset of Fig. 7(B).

Let us also analyze the influence of the inhibition mechanism and the release of LGF's on the irrigation of the hypoxic tissue, which will be done by measuring the length of the tissue irrigated after a fixed number N_f of capillaries arrives at the tissue surface. For this purpose, we defined the irrigation length (l_I) as the distance between the most distant irrigated sites of the tissue. Since it is convenient to normalize this quantity by the tissue length m, one actually has the irrigation fraction, i.e., $\nu_I = l_I/m$. In this way, a useful quantity is the probability distribution, $P(\nu_I)$, which gives the occurrence frequency for each value of ν_I, obtained by considering a large number of independent simulations, n_S.

In order to study the effect of both the neighboring inhibition mechanism and the release of LGF's on the irrigation fraction, Fig. 8 depicts the distribution $P(\nu_I)$ as obtained for four different situations. In Fig. 8(A) we show two curves that correspond to $P(\nu_I)$ in the presence and in the absence of the neighboring inhibition mechanism when the release of LGF's is neglected. In Fig. 8(B) we can also see two curves, corresponding to $P(\nu_I)$ in the presence and in the absence of the neighboring inhibition mechanism when LGF's are released.

Let us first study the effect of the neighboring inhibition mechanism on the irrigation length. One observes an important shift of the distribution $P(\nu_I)$ toward a larger irrigation fraction caused by the inhibition mechanism. This effect is apparent

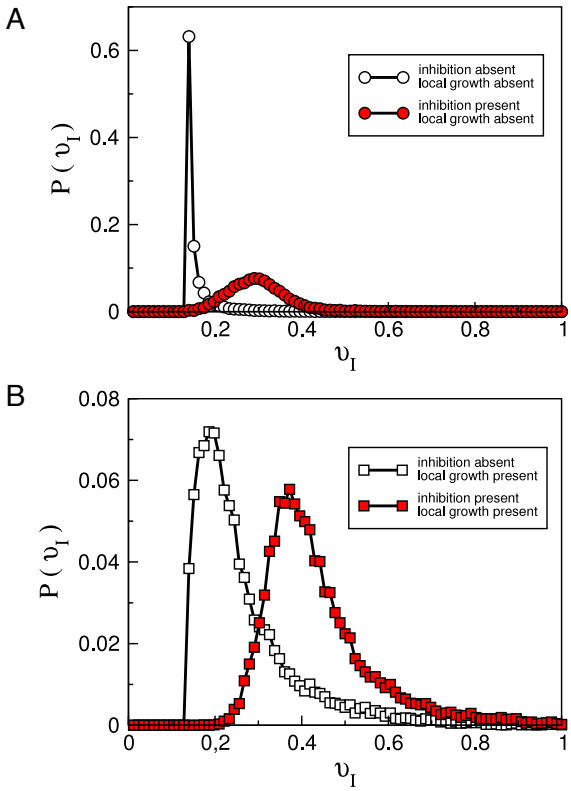

Fig. 8. (Colors on line.) *Irrigation of the hypoxic tissue*. Probability distribution of the irrigation fraction ($P(\nu_I)$) after a fixed number N_f of capillaries arrive at the tissue surface. Effect of the neighboring inhibition mechanism when (A) the release of LGF's is neglected, and (B) the release of LGF's is present. The presence and the absence of the neighboring inhibition mechanism corresponds to filled red symbols and empty symbols, respectively, whereas circles and squares correspond, respectively, to the absence and presence of LGF's. More details in the text. Simulation conditions: $m = 86$, $L = 128$, $M = 256$, $N_f = 12$, and $n_S = 10{,}000$.

both in the absence and presence of the LGF's (Fig. 8(A) and (B), respectively). Since the neighboring inhibition mechanism acts at the surface of the tissue it should affect the irrigation length, as it is, in fact, observed. Besides, with the aid of the distribution function one can also evaluate the average irrigation fraction ($\langle \nu_I \rangle$). When the release of LGF's is neglected (Fig. 8(A)) its value increases from $\langle \nu_I \rangle = 0.155 \pm 0.038$ up to $\langle \nu_I \rangle = 0.299 \pm 0.070$ when the neighboring inhibition mechanism is considered. A rather similar behavior is observed when the release of LGF's is introduced (Fig. 8(B)). Here, an enhancement of the average irrigation fraction from $\langle \nu_I \rangle = 0.26 \pm 0.12$ up to $\langle \nu_I \rangle = 0.43 \pm 0.12$ is also found due to the incorporation of the neighboring inhibition mechanism.

It is worth mentioning that there is a minimum limit in the irrigation length, which would occur if the total number of capillaries (N_f, fixed for all simulations considered) may arrive at the surface tissue along a single compact line. This results in a minimum irrigation fraction, N_f/m, approximately equal to 0.1395 for the parameters used in Fig. 8. Owing to the existence of this minimum irrigation fraction there is an asymmetry in the distributions when the neighboring inhibition mechanism is absent. Particularly, for the case without LGF's and with the neighboring inhibition mechanism absent, the most probable irrigation length, that is, the mode of the distribution, is exactly 0.1395, as one can see from Fig. 8(A) (curve with empty circles).

In order to understand these results, one should remember that for the case without the neighboring inhibition mechanism, when the growing capillary network gets in contact with the hypoxic tissue, only the irrigated site becomes inhibited for the release of GF's. Therefore the subsequent capillaries that will reach the hypoxic tissue will most probably be the neighboring sites of the first one, since these sites are still active for the release of GF's. On the other hand, if the inhibition mechanism is present, when the growing capillary network reaches the hypoxic tissue, five neighboring sites become inhibited for the release of GF's (the contact site, as well as two additional sites on each side of it). Because GF's continue to be released by the other active sites, the growing network will most probably grow in the direction of these active sites, resulting in a larger irrigation fraction when the inhibition mechanism is present, since the simulations are always performed until a fixed number of capillaries arrive at the tissue surface. Also, when the neighboring inhibition mechanism is considered, the asymmetry arising from the minimum irrigation fraction is less evident, since greater irrigation lengths are expected, as observed in both Fig. 8(A) and (B).

Let us now study the effect of LGF's on the irrigation length. It is worth noting that the relative difference in $\langle \nu_I \rangle$ due to the presence of the neighboring inhibition mechanism is more pronounced when LGF's are absent (Fig. 8(A)), as compared with the case when LGF's are present (Fig. 8(B)). In the latter situation, the release of LGF's blurs the gradient generated by the

hypoxic tissue and, consequently, the effect of the neighboring inhibition mechanism on this gradient is less evident. Besides, one can see an enhancement of the average irrigation fraction $\langle \nu_I \rangle$ caused by the release of LGF's, in the absence of the neighboring inhibition mechanism, just by comparing the curves with empty circles and empty squares of Fig. 8(A) and (B), respectively. A quite similar behavior is found when the neighboring inhibition mechanism is considered (that is, comparing the curve with filled red circles of Fig. 8(A) and the curve with filled red squares of Fig. 8(B)). In order of understand these results, one can argue that the presence of LGF's disturbs the gradient generated by the hypoxic tissue and, consequently, reduces the directionality of the growing capillaries (as we showed in Fig. 4), generating a denser and more tortuous network. This effect allows different branches of the growing network to get in contact with the hypoxic tissue (as can be seen in Fig. 3), resulting in a shift of the curves presented in Fig. 8 to larger values of the irrigation fraction when LGF's are present.

Another feature to note, related to the marked asymmetry of the distribution of $P(\nu_I)$ for the case where both the release of LGF's and the neighboring inhibition mechanism are absent (curve with empty circles in Fig. 8(A)), is that the probability of occurrence of the minimum irrigation length is remarkably high, ≈ 0.632. When the neighboring inhibition mechanism is considered, also in the absence of LGF's (curve with filled red circles in Fig. 8(A)), the probability of occurrence of the minimum irrigation length is only ≈ 0.003. Note that the presence of the neighboring inhibition mechanism does not allow the release of GF's from the inhibited sites, but it is possible that capillaries would get in contact with these blocked sites (although it is unlikely, as discussed before), therefore the minimum irrigation length can also be found in this case. This abrupt change can be understood by remembering that the neighboring inhibition mechanism acts at the surface of the hypoxic tissue generating a larger irrigation fraction. On the other hand, when LGF's are released and the neighboring inhibition mechanism is absent (curve with empty squares in Fig. 8(B)), the probability of occurrence of the minimum irrigation length is ≈ 0.038. In this case, one can also observe an important decrease in the probability of the occurrence of the minimum irrigation length, but now related to the effect caused by the release of LGF's on the shape of the capillary network, which also results in a larger irrigation fraction.

Summarizing, from Fig. 8 we conclude that the best irrigation of the hypoxic tissue can be achieved when both the neighboring inhibition mechanism and the LGF's are considered (curve with filled red squares in Fig. 8(B)), since it presents higher values of the average irrigation fraction $\langle \nu_I \rangle$. In this situation, one has both the effect of the neighboring inhibition mechanism raising the irrigation length and the effect of the LGF's, which affects the shape of the capillary network and, consequently, also contributes to obtaining larger irrigation fractions.

4. Discussion

In this work we studied a lattice model for the description of angiogenesis. We analyze the effect of both the release of LGF's and the neighboring inhibition mechanism on properties such as the directionality of the growing network and the degree of irrigation of the hypoxic tissue, in order to obtain a better description and understanding of the angiogenesis process. Our model is based on an early work by Gazit et al. [18], with an extension in order to include the inhibition mechanism, i.e., a fixed number of neighboring sites of an already irrigated site of the hypoxic tissue stop releasing growth factors due to the arrival of nutrients. It is worth saying that by using a circular geometry for the release of GF's, as used by Gazit et al. [18], it is not possible to study the directionality of the growing network. Also, Gazit et al. do not study the irrigation process since they do not consider the contact of the capillary network with the hypoxic tissue.

In normal angiogenesis one expects that the capillary network will be directional in order to correctly attend to the nutrient demand of a particular hypoxic region of a tissue. Our results show that the directionality of the growing network is more evident when LGF's are absent (cf. Fig. 4). Besides, the neighboring inhibition, which is proposed here as a control mechanism, is also expected to play a key role in normal angiogenesis. From Fig. 8 we show that a better irrigation of the hypoxic tissue can be achieved when the neighboring inhibition mechanism is considered, since for these situation one has higher values of the average irrigation fraction $\langle \nu_I \rangle$. In fact, in normal angiogenesis one expects an efficient irrigation of the hypoxic tissue. Therefore, one could relate the model studied here in the absence of LGF's and with the neighboring inhibition mechanism present, to a normal angiogenesis process. In this situation the model provides a directional capillary network and a good irrigation of the hypoxic tissue. Also, from Fig. 3(B) one can see a relatively ordered capillary network, in agreement with experimental results for normal angiogenesis [23,34]. However, the existence of LGF's that can be associated with a local amplification of the signal generated by the hypoxic tissue, accounting for the regulation of the cells of the capillaries on the shape of the growing network, seems to be an ingredient that should be present in a description of normal angiogenesis. Therefore we expected that by considering a small number of LGF's in our model one should still obtain a directional network, that could be related in a more suitable way (since this control mechanism would be present) with a normal angiogenesis process.

On the other hand, in tumor angiogenesis one would expect that control mechanisms, such as the neighboring inhibition proposed here, will not be operative. Also, a large number of released LGF's could also be related to a tumor angiogenesis, indicating the absence of cell regulation in the shape of the growing capillary network. Note that the proportion between LGF's and GF's chosen in our model represents this situation, since for each GF released by the hypoxic tissue, one LGF is also released by the growing network. In fact, our results when the release of LGF's is present but the neighboring inhibition mechanism is absent, exhibit rather small directionality for the growing structure (cf. Fig. 4) and with a worse degree of irrigation of the hypoxic tissue (cf. Fig. 8). Besides, from Fig. 3(C), one can see a more tortuous capillary network with many closed branches and loops, in agreement with experimental results [9,23,30,34–36]. Therefore for this situation the model could be appropriate for the description of tumor angiogenesis.

In addition, we can conclude that the neighboring inhibition can be thought of as a local mechanism that preferentially affects the hypoxic tissue (and consequently the irrigation length), whereas the release of LGF's can be thought of as a global mechanism, since it affects all the development of the capillary network, including both its directionality and shape, as well as the irrigation length (cf. Figs. 4 and 8).

Extensions of the present model could be implemented. In that way, besides the presence of stimulators of angiogenesis (growth factors), one could also consider the inhibition of the growing capillary network, through, e.g., endothelial cell death (endogenous inhibition) or for the case of tumor angiogenesis, administered inhibitors of angiogenesis. In that case one could study how the balance between stimulators and inhibitors affects the capillary network or the irrigation of the hypoxic tissue [37]. The endogenous inhibition could also be useful to study vessel remodeling.

In spite that some previous works present only a qualitative analysis of the growing capillary network [17,21,27], the quantification of properties related with angiogenesis can be found in several other works. In that way, simplified models for angiogenesis were proposed to measure fractal dimension and percolation transition properties [18,23,38,39]. When more complex tools are used in modeling, like the combination of continuous and stochastic approaches, the quantification of properties related with network coverage (sprout velocity, branch density, vessel length/diameter, flow rate, etc.) is possible [15,25,40]. In the present work, by means of a simplified model and therefore with only few parameters, we present a quantification of two relevant features for angiogenesis modeling: the directionality of the growing network and the irrigation degree of hypoxic tissue. We recall that by means of these measurements we are able to suggest differences between normal and tumor angiogenesis. We expect that these parameters could contribute to a better characterization of the complex angiogenesis process and stimulate the cross-talking between experimental and theoretical work.

Acknowledgments

We acknowledge financial support from the Argentinian Science Agencies CONICET and ANPCyT, and from the UNLP (Universidad Nacional de La Plata).

References

[1] N. Ferrara, Am. J. Physiol. Cell Physiol. 280 (2001) C1358.
[2] H.F. Dvorak, L.F. Brown, M. Detmar, A.M. Dvorak, Am. J. Pathol. 146 (1995) 1029.
[3] J. Folkman, Curr. Mol. Med. 3 (2003) 643.
[4] G. Bergers, L.E. Benjamin, Nat. Rev. Cancer 3 (2003) 401.
[5] J. Folkman, N. Engl, J. Med. 285 (1971) 1182.
[6] D. Ribatti, History of Research on Tumor Angiogenesis, Springer, Netherlands, 2009.
[7] P. Carmeliet, Nat. Med. 9 (2003) 653.
[8] N. Woolf, Pathology Basic and Systemic, W.B. Saunders, London, 1998.
[9] R.K. Jain, P.F. Carmeliet, Sci. Amer. 285 (2001) 38.
[10] O. Benny, K. Nakai, T. Yoshimura, L. Bazinet, J.D. Akula, et al., PLoS ONE 5 (9) (2010) e12515.
[11] A. Tandle, D.G. Blazer, S.K. Libutti, J. Transl. Med. 2 (2004) 22.
[12] L. Hlatky, P. Hahnfeldt, J. Folkman, J. Natl. Cancer Inst. 94 (2002) 883.
[13] G. Taraboletti, R. Giavazzi, Eur. J. Cancer 40 (2004) 881.
[14] L. Preziosi (Ed.), Cancer Modelling and Simulation, Chapman & Hall, CRC Press, 2003.
[15] R.D.M. Travasso, E. Corvera Poiré, M. Castro, J.C. Rodríguez-Manzaneque, A. Hernández-Machado, PLoS ONE 6 (5) (2011) e19989.
[16] H.A. Levine, S. Pamuk, B.D. Sleeman, M. Nilsen-Hamilton, Bull. Math. Biol. 63 (2001) 801;
H.A. Levine, B.D. Sleeman, M. Nilsen-Hamilton, J. Math. Biol. 42 (2001) 195.
[17] A.R.A. Anderson, M.A.J. Chaplain, Bull. Math. Biol. 60 (1998) 857.
[18] Y. Gazit, D.A. Berk, M. Leunig, L.T. Baxter, R.K. Jain, Phys. Rev. Lett. 75 (1995) 2428.
[19] B. Mohammadi, V. Haghpanah, B. Larijani, Comput. Biol. Med. 38 (2008) 1007.
[20] V. Capasso, D. Morale, J. Math. Biol. 58 (2009) 219.
[21] S. Tong, F. Yuan, Microvasc. Res. 61 (2001) 14.
[22] V. Capasso, A. Micheletti, D. Morale, Math. Biosci. 214 (2008) 20.
[23] J.W. Baish, T. Stylianopoulos, R.M. Lanning, W.S. Kamoun, D. Fukumura, L.L. Munn, R.K. Jain, Proc. Natl. Acad. Sci. USA 108 (2011) 1799.
[24] A. Shirinifard, J.S. Gens, B.L. Zaitlen, N.J. Popławski, M. Swat, et al., PLoS ONE 4 (10) (2009) e7190.
[25] A.L. Bauer, T.L. Jackson, Y. Jiang, PLoS Comput. Biol. 5 (7) (2009) e1000445.
[26] A.L. Bauer, T.L. Jackson, Y. Jiang, Biophys. J. 92 (2007) 3105.
[27] B.D. Sleeman, I.P. Wallis, Math. Comput. Modelling 36 (2002) 339.
[28] M.J. Plank, B.D. Sleeman, P.F. Jones, J. Theoret. Biol. 229 (2004) 435.
[29] M.J. Plank, B.D. Sleeman, Math. Med. Biol. 20 (2003) 135.
[30] M. Leunig, F. Yuan, M.D. Menger, Y. Boucher, A.E. Goetz, K. Messmer, R.K. Jain, Cancer Res. 52 (1992) 6553.
[31] T.A. Witten, L.M. Sander, Phys. Rev. Lett. 47 (1981) 1400.
[32] A.L. Barabasi, H.E. Stanley, Fractal Concepts in Surface Growth, Cambridge University Press, Cambridge, 1995.
[33] E. Ben-Jacob, O. Schochet, A. Tenenbaum, I. Cohen, A. Czirók, et al., Nature 368 (1994) 46.
[34] R.K. Jain, T. Stylianopoulos, Nat. Rev. Clin. Oncol. 7 (2011) 653.
[35] B.J. Vakoc, et al., Nat. Med. 15 (2009) 1219.
[36] V. Muthukkaruppan, R. Auerbach, Science 205 (1979) 1416.
[37] P. Hahnfeldt, D. Panigrahy, J. Folkman, L. Hlatky, Cancer Res. 59 (1999) 4770.
[38] J.W. Baish, R.K. Jain, Cancer Res. 60 (2000) 3683.
[39] A. Gamba, D. Ambrosi, A. Coniglio, A. de Candia, S. Di Talia, E. Giraudo, G. Serini, L. Preziosi, F. Bussolino, Phys. Rev. Lett. 90 (2003) 118101-1.
[40] T.W. Secomb, J.P. Alberding, R. Hsu, M.W. Dewhirst, A.R. Pries, PLoS Comput. Biol. 9 (3) (2013) e1002983.